



日本原子力研究開発機構機関リポジトリ
Japan Atomic Energy Agency Institutional Repository

Title	Resonant photoemission spectroscopy study of impurity-induced melting in Cr- and Ru-doped $\text{Nd}_{1/2}\text{A}_{1/2}\text{MnO}_3$ (A=Ca,Sr)
Author(s)	Kang J.-S., Kim J. H., Sekiyama Akira, Kasai Shuichi, Suga Shigemasa, Han S. W., Kim K. H., Choi E. J., Kimura Tsuyoshi, Muro Takayuki, Saito Yuji, Olson C. G., Shim J. H., Min B. I.
Citation	Physical Review B,68(1),p.012410_1-012410_4
Text Version	Publisher's Version
URL	https://jopss.jaea.go.jp/search/servlet/search?25028
DOI	http://dx.doi.org/10.1103/PhysRevB.68.012410
Right	©2003 The American Physical Society

Resonant photoemission spectroscopy study of impurity-induced melting in Cr- and Ru-doped $\text{Nd}_{1/2}\text{A}_{1/2}\text{MnO}_3$ ($A = \text{Ca}, \text{Sr}$)

J. -S. Kang,¹ J. H. Kim,¹ A. Sekiyama,² S. Kasai,² S. Suga,² S. W. Han,³ K. H. Kim,³ E. J. Choi,⁴ T. Kimura,⁵ T. Muro,⁶ Y. Saitoh,⁷ C. G. Olson,⁸ J. H. Shim,⁹ and B. I. Min⁹

¹*Department of Physics, The Catholic University of Korea, Puchon 420-743, Korea*

²*Department of Material Physics, Graduate School of Engineering Science, Osaka University, Osaka 560-8531, Japan*

³*Department of Physics, Gyeongsang National University, Chinju 660-701, Korea*

⁴*Department of Physics, The University of Seoul, Seoul 130-743, Korea*

⁵*Department of Applied Physics, University of Tokyo, Tokyo 113-0033, Japan*

⁶*JASRI, SPring-8, Hyogo 679-5198, Japan*

⁷*Department of Synchrotron Radiation Research, JAERI, SPring-8, Hyogo 679-5148, Japan*

⁸*Ames Laboratory, Iowa State University, Ames, Iowa 50011, USA*

⁹*Department of Physics, Pohang University of Science and Technology, Pohang 790-784, Korea*

(Received 12 May 2003; published 28 July 2003)

Electronic structures of very dilute Cr- or Ru-doped $\text{Nd}_{1/2}\text{A}_{1/2}\text{MnO}_3$ (NAMO) ($A = \text{Ca}, \text{Sr}$) manganites have been investigated using the Mn and Cr $2p \rightarrow 3d$ resonant photoemission spectroscopy (PES). All the Cr- and Ru-doped NAMO systems exhibit the clear metallic Fermi edges in the Mn e_g spectra near E_F , consistent with their metallic ground states. The Cr $3d$ states with t_{2g}^3 configuration are at ~ 1.3 eV below E_F , and the Cr e_g states do not participate in the formation of the band near E_F . Cr- and Ru-induced ferromagnetism and insulator-to-metal transitions can be understood based on their measured electronic structures.

DOI: 10.1103/PhysRevB.68.012410

PACS number(s): 75.47.De, 79.60.-i, 71.30.+h

The Mn-site doping by magnetic cations, such as Cr, Ru, is known to be a very efficient method to induce metallicity and ferromagnetism in the insulating and antiferromagnetic (AFM) $\text{Nd}_{1/2}\text{A}_{1/2}\text{MnO}_3$ (NAMO) ($A = \text{Ca}, \text{Sr}$).¹⁻⁴ Undoped NAMO has the charge/orbital ordered (CO/OO) quarter-filled insulating phase with the CE-type AFM spin ordering. By doping Ru to NAMO, the Curie temperature T_C is even enhanced.⁵ To explain the Cr-induced insulator-to-metal ($I-M$) transition, the relaxor-ferromagnet has been proposed,⁴ in which the field-induced $I-M$ transition takes place due to the growth of ferromagnetic (FM) microclusters in a matrix of CO/OO state. On the other hand, two valence states of Ru ions are proposed to explain the Ru-induced ferromagnetism.⁶ However, these proposals have not been proved yet and the different behavior of Cr and Ru doping is not well understood.

To explore the melting mechanism of CO/OO in these systems, the main issues to be resolved are (i) the valence and spin states of impurities and (ii) the role of impurities in the metallic band formation. Photoemission spectroscopy (PES) provides direct information on the electronic structures of the CO manganites.^{7,8} In this paper, we report the *bulk-sensitive*⁹ high-resolution valence-band photoemission spectroscopy study for Cr- and Ru-doped NAMO manganites, including resonant photoemission spectroscopy (RPES)⁸⁻¹⁰ near the Mn and Cr $2p$ and Nd $4d$ and $3d$ absorption edges. Using the large resonance enhancement in the $2p \rightarrow 3d$ RPES,⁸ we were able to measure clearly the Cr $3d$ emission for a very dilute Cr-doped system $\text{Nd}_{1/2}\text{A}_{1/2}\text{Mn}_{1-y}\text{Cr}_y\text{O}_3$ ($A = \text{Ca}, \text{Sr}$; $y = 0.05, 0.07$), corresponding to only ~ 1 at.%. Therefore this work opens up the possibility of directly observing the local electronic structure of very dilute transition-metal systems. Furthermore, our PES measurements for a wide photon energy

($h\nu$) range ($h\nu \approx 20$ eV–1000 eV) allow us to determine various partial spectral weight distributions (PSWs) by using the cross-section effect over a wide $h\nu$ range. We have also made a comparison with the Ru-doped $\text{Nd}_{1/2}\text{Sr}_{1/2}\text{Mn}_{1-y}\text{Ru}_y\text{O}_3$ ($y = 0.05$).

$\text{Nd}_{1/2}\text{A}_{1/2}\text{Mn}_{1-y}\text{T}_y\text{O}_3$ ($A = \text{Ca}, \text{Sr}$; $T = \text{Cr}, \text{Ru}$; $0 \leq y \leq 0.1$) were grown using the floating zone method. The details of the crystal growing method is described elsewhere.⁴ High-resolution $T2p \rightarrow 3d$ RPES ($T = \text{Cr}, \text{Mn}$) experiments were performed at the twin-helical undulator beam line BL25SU of SPring-8 equipped with a SCIENTA SES200 analyzer. Samples were fractured and measured in vacuum better than 3×10^{-10} Torr at $T \leq 20$ K. PES data were obtained in the transmission mode, with the overall energy resolution full width at half maximum (FWHM) of about 80 meV at $h\nu \sim 600$ eV. All the spectra were normalized to the photon flux estimated from the mirror current. Low energy PES experiments were carried out at the Ames/Montana beamline at the Synchrotron Radiation Center (SRC). Samples were fractured and measured in vacuum with a base pressure better than 3×10^{-11} Torr and at $T \leq 15$ K with the FWHM ≈ 80 meV at $h\nu \approx 20$ eV. All the samples showed a clean single peak in the O $1s$ core-level spectra and no 9 eV binding energy (BE) peak in the valence-band spectra.

Figure 1 shows the valence-band spectra of Cr- and Ru-doped $\text{Nd}_{1/2}\text{Ca}_{1/2}\text{MnO}_3$ (NCMO) and $\text{Nd}_{1/2}\text{Sr}_{1/2}\text{MnO}_3$ (NSMO) near the Mn and Cr $2p_{3/2}$ absorption edges. Large enhancement in Mn $2p \rightarrow 3d$ RPES for Cr- and Ru-doped NAMO is similar to those of the previous report on CO NSMO.⁸ As to the resonating behavior of the Mn $3d$ -derived states (the left panel), those near ~ 2.3 eV BE and E_F ($0 \sim 1$ eV) are identified as the t_{2g}^3 and e_g^x ($x \approx 0.5$) majority-

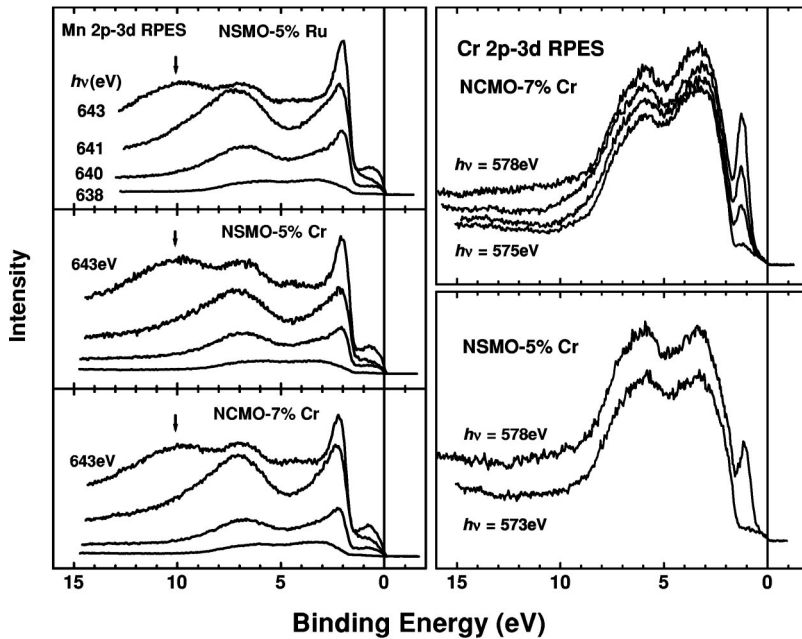


FIG. 1. Left: The Mn $2p \rightarrow 3d$ RPES spectra of NSMO-5% Ru, NSMO-5% Cr, and NCMO-7% Cr around $h\nu \sim 640$ eV. The bump structures below the arrow are the Mn LMM Auger emission. Right: The Cr $2p \rightarrow 3d$ RPES spectra of NCMO-7% Cr and NSMO-5% Cr around $h\nu \sim 575$ eV.

spin states, respectively.^{11,12} These RPES measurements reveal that the high BE features (5–8 eV) also have the large Mn $3d$ electron character, which is strongly hybridized with the O $2p$ electrons. The broad bump around 10 eV BE (denoted by arrow) for $h\nu \sim 643$ eV is due to the Mn LMM Auger emission.

In the right panel, the sharp resonating feature around ~ 1.3 eV BE indicates strong Cr $3d$ character. The absence of the Cr $3d$ electron emission near E_F indicates that doped Cr ions in NCMO and NSMO are in the localized trivalent Cr^{3+} states (t_{2g}^3 configuration), and that Cr e_g states are located above the Mn e_g states. In fact, our Cr $2p$ XAS spectrum of NCMO (not shown here) is very similar to that of a formally trivalent Cr_2O_3 ,¹³ but quite different from those of formally divalent or tetravalent Cr compounds. It thus suggests that Cr e_g states do not participate in the formation of the band near E_F , nor affect the bandwidth of the e_g states near E_F . This feature can be understood based on the previous finding that Cr spins order antiparallel to the Mn subnetwork,¹⁴ and so the hopping between Cr and neighboring Mn ions is not allowed. This conclusion is supported by the comparison of the e_g spectra near E_F in Fig. 3.

Figure 2 compares the valence-band spectra of 7% Cr-doped NCMO for a wide $h\nu$ range ($22 \text{ eV} \leq h\nu \leq 978 \text{ eV}$). The different valence-band line shapes with varying $h\nu$ reflect different contributions from different electron character. Note that these high- $h\nu$ PES spectra can be considered to represent the bulk electronic states.^{9,15} The top three spectra correspond to the on-resonance spectra in the Mn $2p \rightarrow 3d$, Cr $2p \rightarrow 3d$, and Nd $3d \rightarrow 4f$ RPES. Therefore the enhanced features in the top three spectra are due to the Mn $3d$, Cr $3d$, and Nd $4f$ electron emissions.

If one assumes Nd^{3+} ($4f^3$), $\text{Mn}^{3.5+}$ ($3d^3 - 3d^4$), and the filled O $2p$ bands ($2p^6$) in NCMO, and ignores the resonance effect, then the cross-section ratio of Nd $4f$: Mn/Cr $3d$: O $2p$ electrons per unit cell is about $\sim 1\% : \sim 8\% : \sim 92\%$ at $h\nu \approx 22$ eV, $\sim 16\% : \sim 27\% : \sim 57\%$ at $h\nu$

≈ 120 eV, and $\sim 48\% : \sim 24\% : \sim 28\%$ at $h\nu \approx 640$ eV.¹⁶ Therefore the $h\nu = 22$ eV spectrum can be considered as the O $2p$ PSW. In the $h\nu = 22$ eV spectra, open circles and gray lines denote that for 2% Cr-doped NSMO and 4% Cr-doped NCMO, respectively. The similar line shapes at $h\nu = 22$ eV indicate that the O $2p$ states are very similar in Cr-doped NAMO manganites. As $h\nu$ increases, the Mn $3d$ and Nd $4f$ emissions increase with respect to the O $2p$ emission, and the Mn $3d$ and O $2p$ emissions become comparable to each

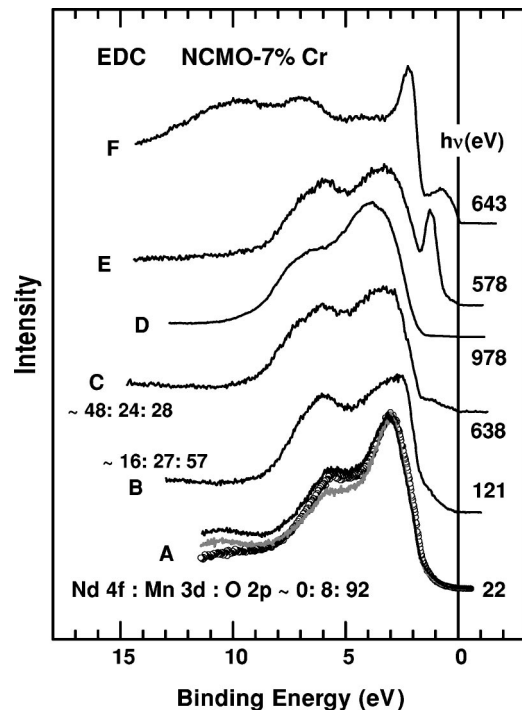


FIG. 2. Valence-band spectra of NCMO-7% Cr for $22 \text{ eV} \leq h\nu \leq 978 \text{ eV}$. The spectra are scaled to have approximately the same area.

other at $h\nu \approx 638$ eV (the Mn $2p \rightarrow 3d$ off resonance). In fact, we have observed that the overall features of Cr- and Ru-doped NAMO ($A = \text{Ca}, \text{Sr}$) are very similar at $h\nu = 638$ eV, and that the valence band widths for NCMO systems are slightly narrower than those for NSMO systems,¹⁷ which is consistent with the larger ionic size of Sr than for Ca, causing the electron hopping easier.

The on-resonance spectrum in the Nd $3d \rightarrow 4f$ RPES ($h\nu = 978$ eV) Ref. 18 represents the Nd $4f$ PSW owing to the large resonance enhancement. The Nd $4f$ -derived states exhibit two broad peaks around ~ 4 eV and ~ 7 eV BE, which overlap substantially with the O $2p$ states between 3-6 eV (see the $h\nu = 22$ eV spectrum). No emission is observed near E_F where the Mn e_g bands are located. These observations suggest that Nd $4f$ states are strongly hybridized with the O $2p$ states, but very little with the Mn e_g states. Thus the Nd $4f$ states do not participate in the band formation near E_F . We have found¹⁷ that the Nd $4f$ PSW's of Cr- and Ru-doped NAMO ($A = \text{Ca}, \text{Sr}$), determined from the Nd $4d \rightarrow 4f$ RPES, are essentially the same as one another and also very similar to that determined from the Nd $3d \rightarrow 4f$ RPES. Considering the difference in the electron mean free paths between the Nd $4d \rightarrow 4f$ RPES and the Nd $3d \rightarrow 4f$ RPES, this finding indicates that the *surface* Nd $4f$ states are very similar to the *bulk* Nd $4f$ states in NAMO manganites, which makes a sharp contrast to the case of Ce compounds.¹⁵ We interpret the Nd $4f$ PSW to represent roughly the $4f^3$ ground state, but with the large final-state hybridization to O $2p$ orbitals.^{10,12}

Figure 3 compares the near- E_F regions of the valence-band spectra of Cr- or Ru-doped NCMO and NSMO at $h\nu = 22$ eV (top), at $h\nu = 643$ eV (middle), and at $h\nu = 638$ eV (bottom). The $h\nu \approx 643$ eV spectra (middle), corresponding to the Mn $2p \rightarrow 3d$ RPES, represent the Mn e_g PSW's.^{11,12} At $h\nu \approx 643$ eV, the metallic Fermi edges are clearly observed for all the samples, which is consistent with their metallic ground states. In contrast, the spectral intensity near $E_F[I(E_F)]$ at $h\nu = 22$ eV is very weak in view of the metallic nature of the samples. This difference arises from the fact the O $2p$ emissions are dominant at $h\nu = 22$ eV and that the O p states have a negligible contribution near E_F . This comparison reveals that Mn e_g states play an important role in determining the I - M transition. For comparison, the spectra at the off-resonance energy of the Mn $2p \rightarrow 3d$ RPES ($h\nu \approx 638$ eV) are shown at the bottom, which were obtained with a lower resolution (FWHM ~ 130 meV) than the above spectra (FWHM ~ 80 meV).¹⁹ For all the cases, $I(E_F)$ is lower for the NCMO-based system than for the NSMO-based system, reflecting the stronger metallic nature for NSMO than for NCMO. Note that the larger Cr-doped NSMO exhibits a higher $I(E_F)$ than the smaller Cr-doped NSMO (see $h\nu = 22$ eV), and that the Ru-doped NSMO shows a higher $I(E_F)$ than the Cr-doped NSMO (see $h\nu = 638$ eV). These features are consistent with the observations that the metallic nature increases with the higher Cr doping and that T_C is higher for the Ru-doped NSMO than for the Cr-doped NSMO.

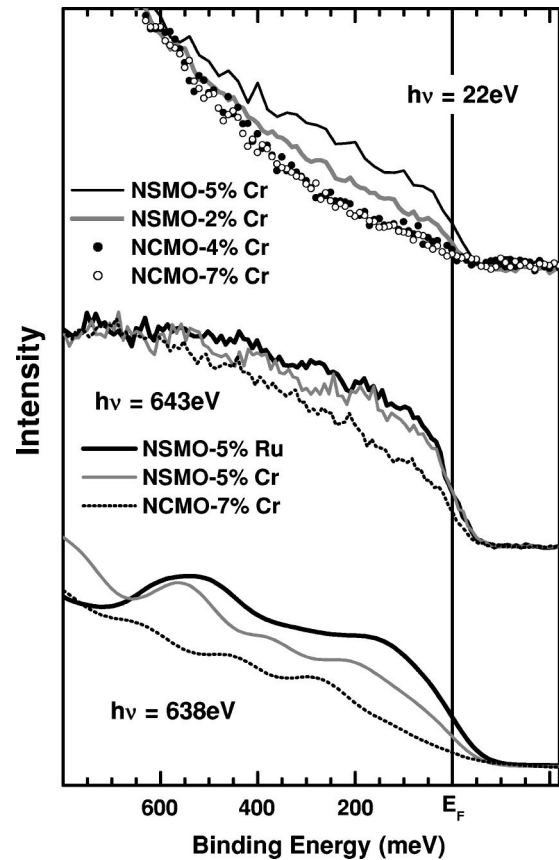


FIG. 3. Near- E_F region of the valence-band spectra of $\text{Nd}_{1/2}\text{A}_{1/2}\text{Mn}_{1-y}\text{T}_y\text{O}_3$ ($A = \text{Ca}, \text{Sr}; T = \text{Cr}, \text{Ru}$) at $h\nu = 22$ eV (top) and at the Mn $2p \rightarrow 3d$ on-resonance ($h\nu \approx 643$ eV) (middle). These spectra were obtained with ~ 80 meV at FWHM. Bottom: the Near- E_F spectra at the Mn $2p \rightarrow 3d$ off resonance ($h\nu \approx 638$ eV), obtained with ~ 150 meV at FWHM. The spectra are scaled at the peak maxima for each $h\nu$.

Now let us discuss the mechanism of the I - M transition in Cr- and Ru-doped NAMO, based on our observations. The undoped CO/OO NAMO is expected to have the ordered $\text{Mn}^{3+}/\text{Mn}^{4+}$ ($3d^4/3d^3$) configuration with the CE-type AFM spin ordering. We have found that Cr t_{2g} states are located well below E_F , resulting in the trivalent Cr^{3+} state (d^3), as shown in the schematic diagram for the local density of states (Fig. 4). Then the substitution of a Cr^{3+} (d^3) for a Mn^{3+} (d^4) site in the CO/OO NAMO will correspond to the hole filling in the undoped NAMO, and it will play a role similar to the substitution of a Mn^{4+} ion for a Mn^{3+} ion. So one can simply conjecture that these extra carriers, caused by the impurity doping, break the commensurate quarter-filled CO/OO state²⁰ and transform the CO/OO insulating phase into the metallic phase. For example, according to the phase diagram of NSMO, the CO/OO insulating phase of half-doped NSMO with the CE-type AFM is transformed into the metallic A-type AFM with increasing the hole concentration.^{21,22} Similarly, one can infer that the substitution of Ru^{4+} (d^4) into a Mn^{4+} (d^3) site will correspond to the electron filling, and so the CO/OO insulating phase of half-doped NSMO is transformed into the metallic FM phase.

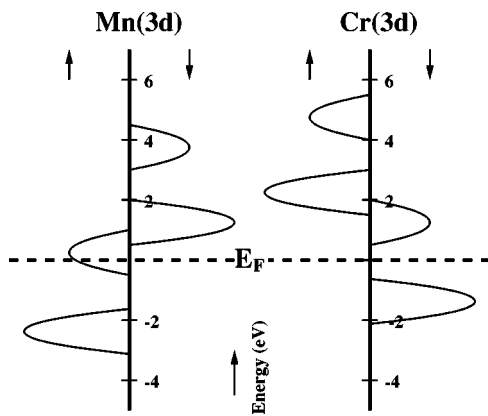


FIG. 4. Schematic local density of states of Mn and Cr for Cr-doped NAMO.

The above picture of the filling control, however, is not complete since Cr-doped NSMO is not A-type AFM but FM. Moreover, NCMO which is the stronger CO system would not exhibit the metallic phase merely with the filling control. Hence it is likely that not only the valence state but also the spin state and the electronic structure are important. The localized spin of Cr^{3+} affects the spin ordering. The AFM superexchange (SE) interaction between Cr^{3+} and neighboring Mn^{4+} ions will give rise to the so-called *domino effect* of reversing the spin directions of $\text{Mn}^{3+}/\text{Mn}^{4+}$ in the FM zig-zag chain of the CE-type AFM.⁶ Likewise, the FM SE interaction between Ru^{4+} and neighboring Mn^{3+} ions also gives rise to the domino effect of reversing the spin directions of $\text{Mn}^{3+}/\text{Mn}^{4+}$. In addition, since Cr^{3+} is not a Jahn-Teller active ion, it will behave as a defect for the OO and the hopping strength around Cr ions will be enhanced due to the reduced Jahn-Teller polaron narrowing effect. Thus the metallic phase could be formed even in NCMO at least around Cr ions, if the double-exchange (DE) hopping strength be-

comes larger than the AFM SE interaction^{21,22} or the hopping strength is larger than the intersite Coulomb interaction between carriers.²³ This picture is consistent with the concept of relaxor-ferromagnet.⁴ In the metallic phase, however, Cr^{3+} itself does not participate in the DE mechanism because two configurations of $\text{Mn}^{3+}-\text{Cr}^{3+}$ and $\text{Mn}^{4+}-\text{Cr}^{2+}$ are not degenerate, as observed in the PES above. That is, the doped Cr^{3+} ion would just initiate the hopping of carriers in the system.

In conclusion, the electronic structures of very dilute Cr- and Ru-doped NAMO have been investigated by employing RPES. The large resonance enhancement in the $2p \rightarrow 3d$ RPES allows us to observe clearly the Cr 3d emission in very dilute (~ 1 at. %) Cr-doped NAMO. The Cr 3d states are observed at ~ 1.3 eV below E_F , corresponding to the t_{2g}^3 configuration of Cr^{3+} ions, which suggests that Cr e_g states do not participate in the formation of the band near E_F . All the Cr- and Ru-doped NAMO systems exhibit the clear metallic Fermi edges in the Mn e_g spectra near E_F , consistent with their metallic ground states. The spectral intensity at E_F is higher for the NSMO-based system than for the NCMO-based system. Further, Ru-doped NSMO has higher spectral intensity near E_F than Cr-doped NSMO, consistent with a higher T_C for Ru-doped NSMO. The melting mechanism in the Cr- and Ru-doped NAMO can be understood first with the concept of the hole and electron filling, respectively, breaking the commensurate CO quarter-filled state. On top of it, the SE interactions between Mn and impurity Cr/Ru ions as well as the enhanced hopping strength due to the reduced Jahn-Teller polaron effect of $\text{Cr}^{3+}/\text{Ru}^{4+}$ ions are expected to yield the metallic ferromagnetism.

This work was supported by the KRF (Grant No. KRF-2002-070-C00038) and by the KOSEF through the CSCMR at SNU and the eSSC at POSTECH. PES experiments were performed at the SPring-8 (JASRI Grant No. 2001B0028-NS-np) and at the SRC (NSF Grant No. DMR-0084402).

- ¹B. Raveau, A. Maignan, and C. Martin, *J. Solid State Chem.* **130**, 162 (1997).
- ²A. Barnabé *et al.*, *Appl. Phys. Lett.* **71**, 3907 (1997).
- ³Y. Moritomo *et al.*, *Phys. Rev. B* **60**, 9220 (1999).
- ⁴T. Kimura *et al.*, *Phys. Rev. Lett.* **83**, 3940 (1999); *Phys. Rev. B* **62**, 15 021 (2000).
- ⁵A. Maignan *et al.*, *J. Appl. Phys.* **89**, 500 (2001).
- ⁶C. Martin *et al.*, *Phys. Rev. B* **63**, 174402 (2001).
- ⁷A. Chainani *et al.*, *Phys. Rev. B* **56**, R15 513 (1997).
- ⁸A. Sekiyama *et al.*, *Phys. Rev. B* **59**, 15 528 (1999).
- ⁹J.-S. Kang *et al.*, *Phys. Rev. B* **66**, 113105 (2002).
- ¹⁰S. Suga *et al.*, *Phys. Rev. B* **52**, 1584 (1995).
- ¹¹J.-H. Park *et al.*, *Phys. Rev. Lett.* **76**, 4215 (1996).
- ¹²J.-S. Kang *et al.*, *Phys. Rev. B* **60**, 13 257 (1999).
- ¹³C. Theil *et al.*, *Phys. Rev. B* **59**, 7931 (1999).
- ¹⁴O. Toulemonde *et al.*, *J. Appl. Phys.* **86**, 2616 (1999).
- ¹⁵A. Sekiyama *et al.*, *Nature (London)* **403**, 398 (2000).
- ¹⁶J.J. Yeh and I. Lindau, *At. Data Nucl. Data Tables* **32**, 1 (1985).
- ¹⁷J.-S. Kang *et al.* (unpublished).
- ¹⁸The $h\nu=978$ eV spectrum in Fig. 2 is that for NSMO-5% Ru

because we do not have that spectrum for NCMO-7% Cr. However, we have found (Ref. 17) that the Nd 4f PSW is essentially the same for Cr- and Ru-doped NAMO.

- ¹⁹The off-resonance spectra shown at the bottom have been smoothed by using a Gaussian function of 100 meV at FWHM to reduce the signal-to-noise ratio. However, the trend observed in the raw spectra is still maintained.
- ²⁰Half-doped manganites such as $\text{Nd}_{1/2}\text{Ca}_{1/2}\text{MnO}_3$ would have the Mn $d^{3.5}$ electron configuration, and so Mn e_g states are thought to be quarter filled. A few models were proposed to describe the CO/OO ordering for these quarter-filled systems. (See Refs. 21 and 22 below.) If one considers the repulsive intersite Coulomb interaction between carriers and the Jahn-Teller interaction, the real-space ordering of carriers takes place and only the lower e_g states are occupied, resulting in the commensurate CO/OO state.
- ²¹J. van den Brink and D. Khomskii, *Phys. Rev. Lett.* **82**, 1016 (1999).
- ²²B.I. Min, Y.-K. Jo, and M.-S. Kim, *Physica B* **312**, 723 (2002).
- ²³J.D. Lee and B.I. Min, *Phys. Rev. B* **55**, R14 713 (1997).